Original Research

Concurrent Incorporation of Mg^{2+} and Li^{+} Ions into CdO Lattice: A Codoping Approach for Optoelectronic Devices

R. Ganapathi [1,2], T. Arivudainambi [1], S. Sakthivel [1], A.R. Balu [3,*]

[1] PG and Research Department of Physics, Raja Serfoji Govt. College (Affiliated to Bharathidasan University, Tiruchirappalli), Thanjavur, Tamilnadu, India
[2] Department of Physics, Kamadhenu College of Arts & Science, Dharmapuri, Tamilnadu, India
[3] PG and Research Department of Physics, AVVM Sri Pushpam College (Affiliated to Bharathidasan University, Tiruchirappalli), Poondi, Tamilnadu, India
* Correspondence: arbalu757@gmail.com

Received: January4, 2026;Accepted: March13, 2026

Abstract:A novel double doping (Mg+Li) has been performed on spray deposited CdO thin film. The structural, morphological, magnetic and optoelectronic properties of the double doped (Mg+Li), Mg-doped and undoped CdO thin films was studied and reported in this work. Crystallite size of pure CdO decreased from 33 nm to 28 nm with Mg-doping and to 24 nm with (Mg+Li) codoping. With (Mg+Li) codoping, nanosized grains are seen. Optical studies show that transparency of pure CdO increases with Mg and (Mg+Li) codoping and a maximum transmittance of 87 % was realized for the (Mg+Li) codoped film which possess a minimum electrical resistivity of 0.25 $\times 10^{-2}$ Ω-cm with an increased figure of merit value (35.3 x 10^{-2} Ω^{-1}), confirming its utility for optoelectronic devices. Paramagnetic nature of CdO becomes ferromagnetic with (Mg+Li) codoping. Ferromagnetic orderings observed for the (Mg+Li) codoped film might due to super-exchange interactions between Mg^{2+} and Li^{+} ions with Cd^{2+} ions in the CdO lattice.

Keywords:spray technique; codoping; figure of merit; ferromagnetism; optoelectronic devices

1. Introduction

Low electrical resistivity, high transparency, intrinsic carrier concentration, good chemical, thermal stability and high mechanical strength of cadmium oxide (CdO) makes it find applications in photovoltaic cells, LCDs, LEDs, smart windows, etc. [1]. Being adegenerate semiconductor, CdO possess (2.2 – 2.7 eV) band gap energy, n-type conductivity depending on O vacancies and Cd interstitials [2]. However, CdO has certain limitations to be used in optoelectronic devices [3]. To utilize CdO for optoelectronic applications, doping with foreign elements such as Mg [4], Ba [5], Zn [6], Cr [7], etc has been attempted earlier. Besides single doping, double doping has also been tried in the past to enhance CdO's electrical and optical characteristics. Some of the earlier double doped works on CdO are (Li,Ni); (Zn,M (M: Li, Na, K)); (B,H), etc. [8 – 10].

In this work, double doping (Mg+Li) has been attempted on CdO. Both the dopants have different peculiar characteristics which could improve CdO's physical properties. Since magnesium (Mg^{2+}), a transition metal ion with ionic radius of 0.72 Å, electronegativity of 1.31 Paulingwhich is less than that of Cd^{2+} (0.97 Å and 1.69 Pauling) belongs to the same P63/mmc space group as cadmium; it may influence CdO's band gap [4]. Lithium (Li^{+}), a group I cation with an ionic radius

of 0.68 Å and shallowest ionization energy could alter oxide films' physical properties [11]. These characteristics facilitates the ready substitution of Mg^{2+} and Li^{+} ions in the CdO crystal lattice suggesting potential enhancement of its optoelectronic properties through co-doping. In our earlier work Mg and Ag with 2 wt.% doping concentrations showed pronounced impact on CdO's optical, electrical, and optoelectronic properties [RG1]. Regarding CdO's magnetic nature, Ag codoping does not contribute much which limits it suitability for spintronic applications. To overcome this, lithium is added as a codopant to improve the magnetic nature of CdO:Mg thin film.

Hence, by (Mg+Li) codoping CdO's optoelectronic and magnetic properties could be improved. Spray pyrolysis technique has been adapted here to deposit undoped, Mg-doped and (Mg+Li) codoped CdO thin films. The choice of spray pyrolysis method stem from its cost-effectiveness, versatility and precise control over film thickness and doping concentrations. This method is particularly suitable for large-scale industrial implementation. The novelty of this research resides in the fabrication of a double doped CdO film with a fixed concentration of magnesium and lithium, employing the cost-effective spray technique while ensuring structural homogeneity of the deposited (Mg+Li) codoped CdO film.

2. Materials and method

Cadmium acetate, magnesium chloride and lithium chloride all of AR grade are the salts used to deposit U, M and ML thin films. Micro glass slides were used as the substrates.

2.1 Deposition parameters

The parameters used to deposit U, M and ML thin films are compiled in Table 1.

Table 1 Deposition parameters used to deposit U, M and ML thin films.

Parameter	Value
Substrate temperature	400°C
Spray to nozzle distance	25 cm
Spray pressure	12 kg/cm^2
Spray liquid flow rate	2 mL/min
Spray solution volume	50 mL
Spray procedure	5 sprays per second followed by a gap of 20 seconds

2.2 Deposition procedure

Undoped (U), Mg-doped (M) and (Mg+Li) codoped CdO (ML) thin films were deposited by spray pyrolysis technique. To create U film, 0.1 M cadmium acetate diluted in 50 mL deionised water (the starting solution) was sprayed onto heated glass substrates. To the starting solution 2 wt% magnesium chloride was added and sprayed to get M film. Lithium chloride of 2 wt% is added to cadmium acetate and magnesium chloride dissolved solution and sprayed to get (Mg+Li) codoped CdO thin films.

2.3 Characterization

The microstructural parameters were measured using diffractometer (PW 340/60). Surface morphology was analyzed using HITACHI S-3000H microscope. UV-vis-NIR spectrophotometer (LAMBDA-35) was used for optical investigations. Utilising Varian carry Eclipse spectrophotometer, PL investigations were conducted. Electrical and magnetic investigations were done using four point probe setup and vibrating sample magnetometer (Lakshore 7410).

3. Results and discussion

3.1 XRD

Diffraction peaks observed in the U, M and ML films (Fig. 1) fit with CdO's cubic structure (JCPDS Card No. 05-0640).

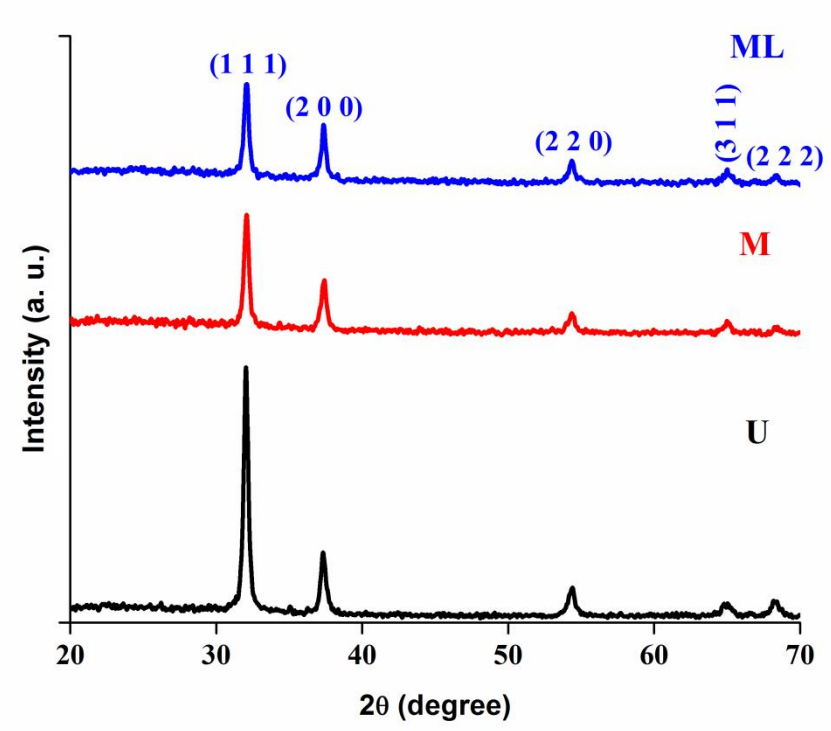

Fig1. U, M and ML's XRD patterns.

All films exhibit (111) preferential orientation. The diffraction peak intensities decreased with Mg-doping and (Mg+Li) codoping which strongly supports for the deterioration in the crystalline quality of pure CdO with the inclusion of dopants [12].

The structural parameters (Table 1) were calculated using the relations [1-4]:

Crystallite size, $D = \frac{0.9\lambda}{\beta cos\theta}$ (1)

Strain, $\varepsilon = \frac{\beta cot\theta}{4}$ (2)

Dislocation density, $\delta = \frac{1}{D^2}$ (3)

Lattice constant, $a = d\sqrt{h^2 + k^2 + l^2}$ (4)

CdO's crystallite size decreased with Mg doping and (Mg+Li) codoping due to Zener pinning effect [14], according to which crystallites growth restriction are caused by crystal defects like vacancies and interstitials.

Table 2. U, M and ML's microstructural parameters.

Film	2θ	β (radian)	D (nm)	$\varepsilon \times 10^{-3}$	$\delta \times 10^{-15}$	a (Å)
U	32.051°	0.2460	33	3.737	0.886	4.8369
M	32.107°	0.2952	28	4.476	1.276	4.8289
ML	32.106°	0.3444	24	5.222	1.736	4.8287

The drag force that dopant ions create on boundary motion and grain formation may also be a contributing factor to the decrease in crystallite sizes [14]. Increased strain values might have decreased M and ML's crystallite size values. Increase strain results from defect clustering, dislocations and grain boundary segregation [15]. Doping and codoping reduced the value of pure CdO's lattice parameter, which may be because Mg^{2+} and Li^{+} ions have smaller ionic radii than Cd^{2+} ions.

3.2 SEM*& EDX*

Fig 2(a-c). shows U, M and ML's SEM images. Grains of varying sizes and shapes make up U film. Bundled grains are also seen.

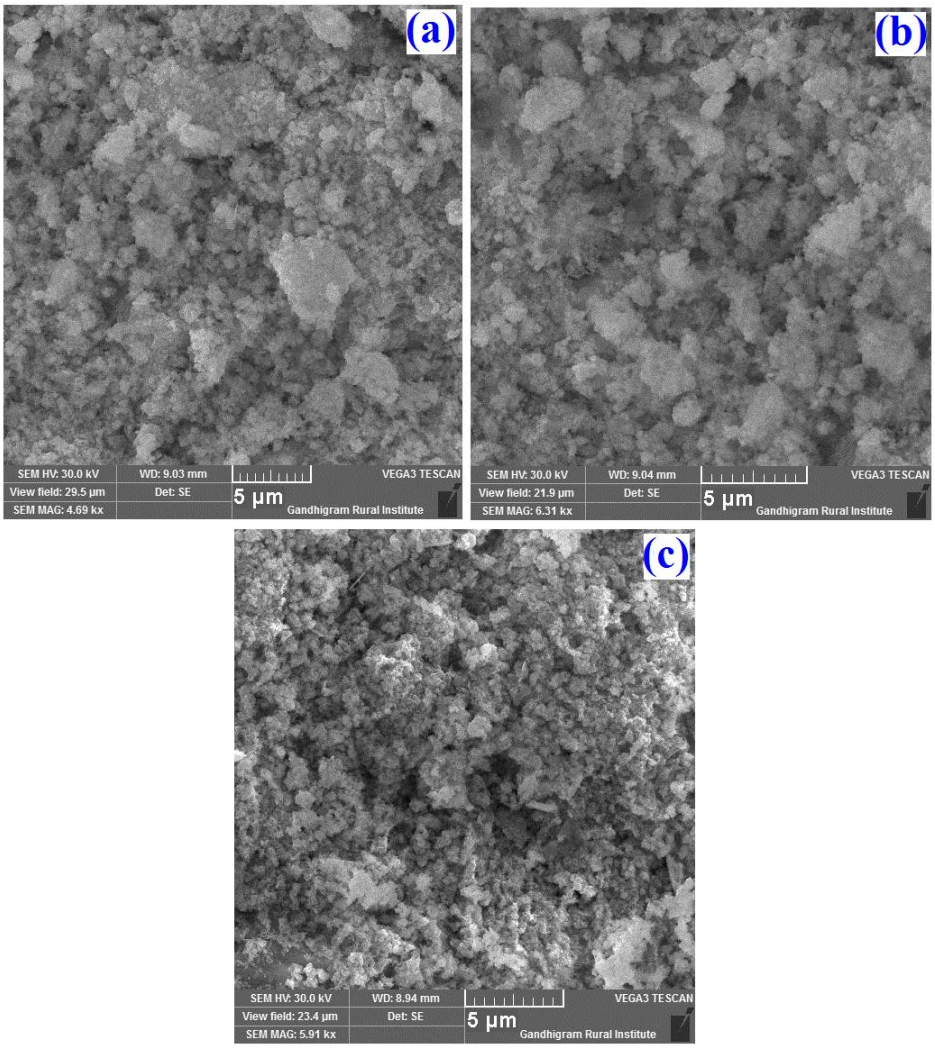

Fig2(a-c). U, M and ML's SEM images.

With Mg doping, grains appear uniform. Agglomerations of grains are observed. With (Mg+Li) codoping, sizes of the grains seem to be uniform and nanosized grains are seen. The grain size of pure CdO decreased with Mg doping and (Mg+Li) codoping which supports the XRD results (Section 3.1). Dopant induced lattice distortion and defect accumulation might have contributed to decreased grain size for the M and ML films.

EDX spectrum of ML film (Fig3.) confirmed the existence of Cd, O and Mg. Li presence could not be detected as the characteristic peak of Li is very weak. Mapping image of ML (Fig 4.) shows the uniform distribution of Cd, O, Mg and Li throughout the film's surface.

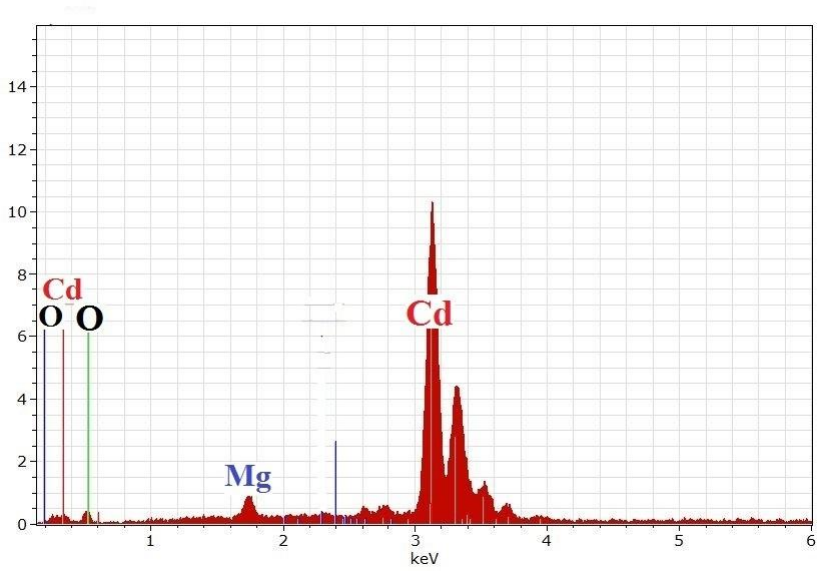

Fig3. EDX spectrum of ML.

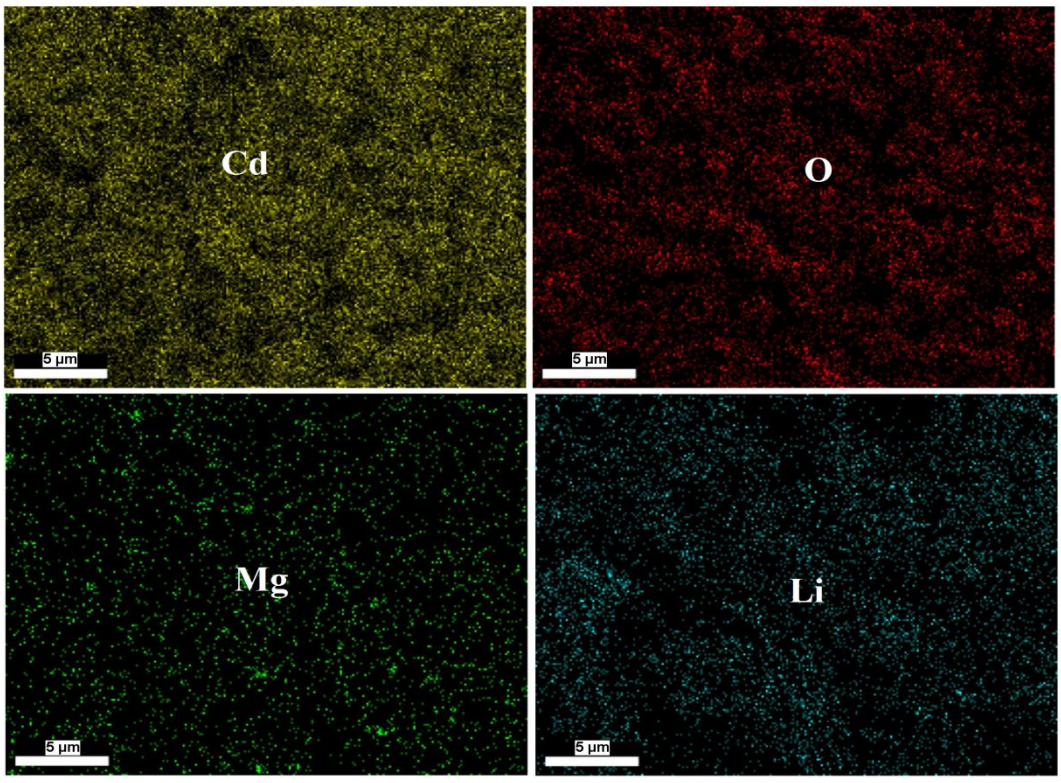

Fig 4. Mapping images of Cd, O, Mg and Li in the ML sample.

3.3 TEM

Nanosized grains were observed for U, M and ML thin films in the TEM images (Fig5.). Grains size of pure CdO decreased with Mg doping and (Mg+Li) codoping which supports XRD and SEM studies.

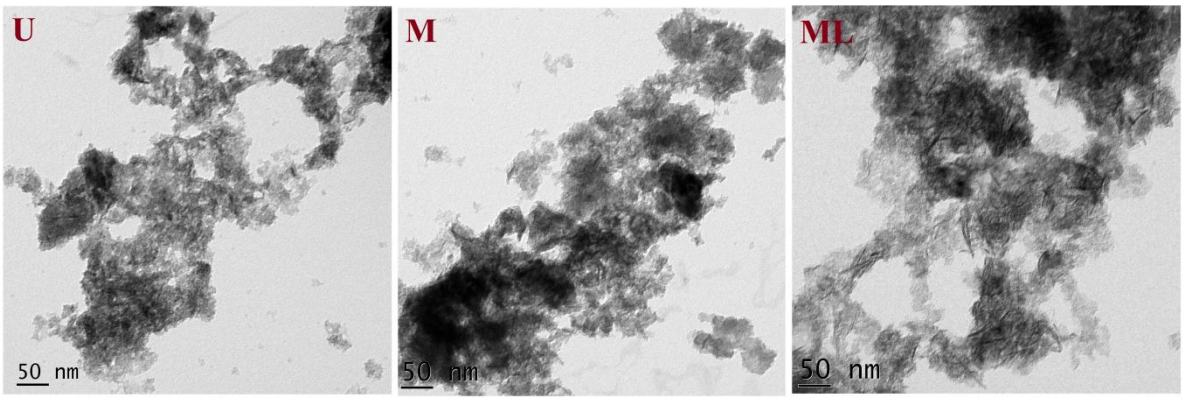

Fig 5. TEM images of U, M and ML films.

3.4 Optical

The transparency of CdO increased with Mg doping and (Mg+Li) codoping (Fig 6.).

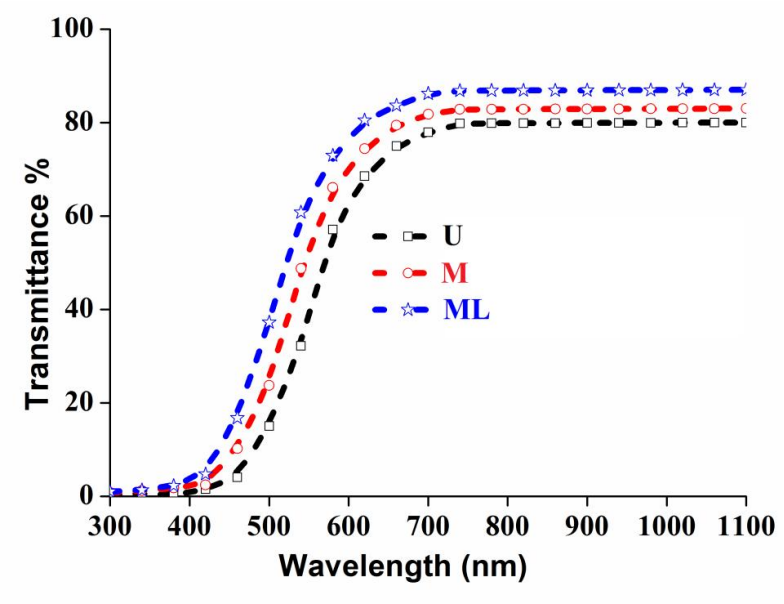

Fig 6.U, M and ML's transmittance spectra

Improved structural homogeneity or fewer scattering flaws may be the cause of the doped and codoped films' increased transparency [16].The M and ML films' absorption edges shifted to lower wavelength side, indicating an increase in their band gaps, E_g as estimated from Fig. 7. U film's $E_g$was found to be 2.44 eV which increased to 2.53 eV for M and then decreased to 2.47 eV for ML film. Band gap widening in M and ML films arises primarily because of the Burstein-Moss effect (BME), where additional free carrier's introduction shifts the Fermi level to the conduction band. This blue shift occurs because the lowest energy states in the conduction band become occupied, necessitating higher energy photons for electron excitation. Furthermore, the ionic radii mismatch between the dopant and host ions induces lattice distortion, altering Cd-O bond lengths and orbit hybridization, which contributes to additional band-edge modification [17]. Increased carrier recombination and trap states also reduces band gap by enabling sub-band transitions.

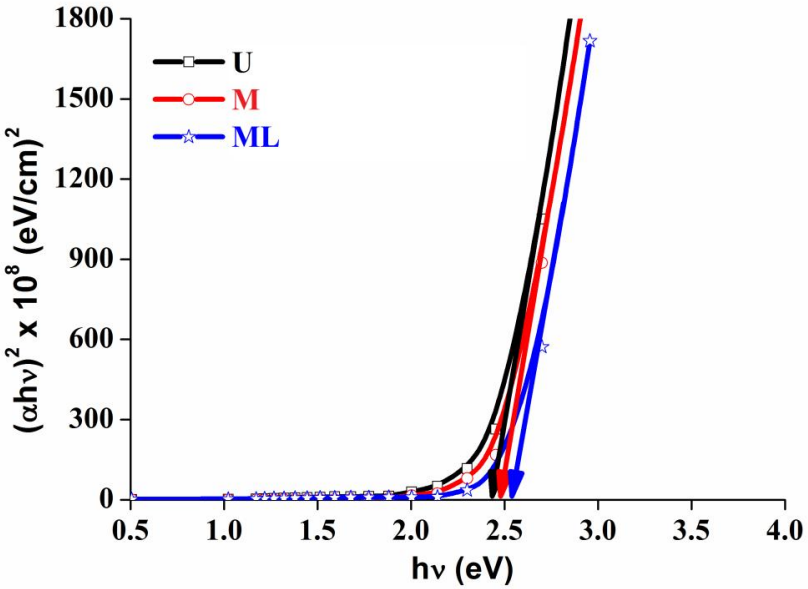

Fig7.U, M and ML's ($\alpha h\nu$)2 vs.$h\nu$ plots.

The quantum confinement effect, in which smaller crystallites cause the band gap to widen, may explain why the absorption edges are shifted to shorter wavelengths in the M and ML films, leading to the larger band gap values [18].

3.5 PL

Pl studies monitor the electronic transition of photoexcited atoms or molecules. The excited atoms make a transition via either radiative or non-radiative processes [19]. In radiative transition, the energy is emitted in the form of photons. PL analysis was carried at room temperature with an excitation wavelength of $\boldsymbol{\lambda}$ = 400 nm, in the wavelength range 450 – 600 nm. Oxygen vacancy defects account for the peak at 460 nm in the PL spectra (Fig 8.) of U, M, and ML thin films [20].The peak at 484 is caused by electrons moving between Cd's interstitial and vacancy states.The 510 nm peak is attributed to donor-acceptor pair [21]. Radiative recombination of photogenerated holes with electrons filling O vacancies on CdO's surface produces the 531 nm peak [22].

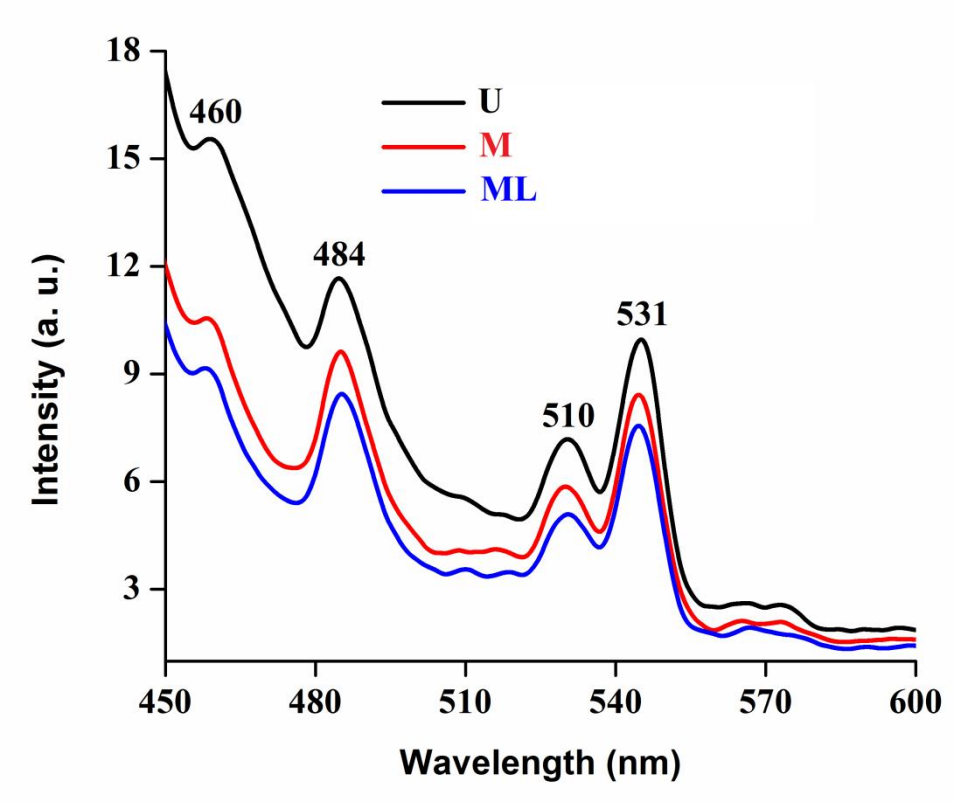

Fig 8.U, M and ML's PL spectra

The lower PL intensities seen in the M and ML films strongly suggest that the recombination rate of electrons and holes photoexcited from them is slower. Because of delayed recombination rate, doped and codoped films are ideal for optoelectronic applications with higher efficiencies.

3.6 Optoelectronic properties

The electrical resistivity values of the U, M and ML films were found to be 2.59 × 10^{-2}, 1.89 × 10^{-2} and 0.25 × 10^{-2}Ω-cm, respectively. Reduced electrical resistivity seen with Mg doping may elevate carrier concentration from enhanced oxygen vacancies caused by the substitutional integration of Mg^{2+} ions into CdO's lattice. The reduced ML's electrical resistivity might be attributed to a reduction in shallow level trap concentration, which increased charge carrier mobility due to reduced electron scattering [23].

Haacke's quality factor (ϕ) or figure of merit (FOM) plays a vital role in determining the suitability of U, M and ML films for optoelectronic applications. It is a quantitative metric for transparent electrodes of PL quantum yield for emitters that evaluate performance by balancing competing factors like optical transmittance, electrical conductivity and efficiency. The figure of merit (ϕ) values were calculated from Eqn. (5):

$$\phi = \frac{T^{10}}{R_{sh}} \qquad (5)$$

where T is the average transmittance in the wavelength regions 400 – 700 nm and R_{sh} is the sheet resistance. The ϕvalues were found to be 1.52, 2.97 and 35.3 × 10^{-2} Ω^{-1} for the U, M and ML films, respectively. Due to increased transmittance and decreased sheet resistance, M and ML

exhibited increased figure of merit values. The high FOM value obtained for ML confirmed its utility for optoelectronic applications.

3.7 VSM studies

Fig 9. shows the M-H curves of U, M and ML thin films. Paramagnetic nature of CdO remains unaltered with Mg doping; however with increased saturated magnetization.

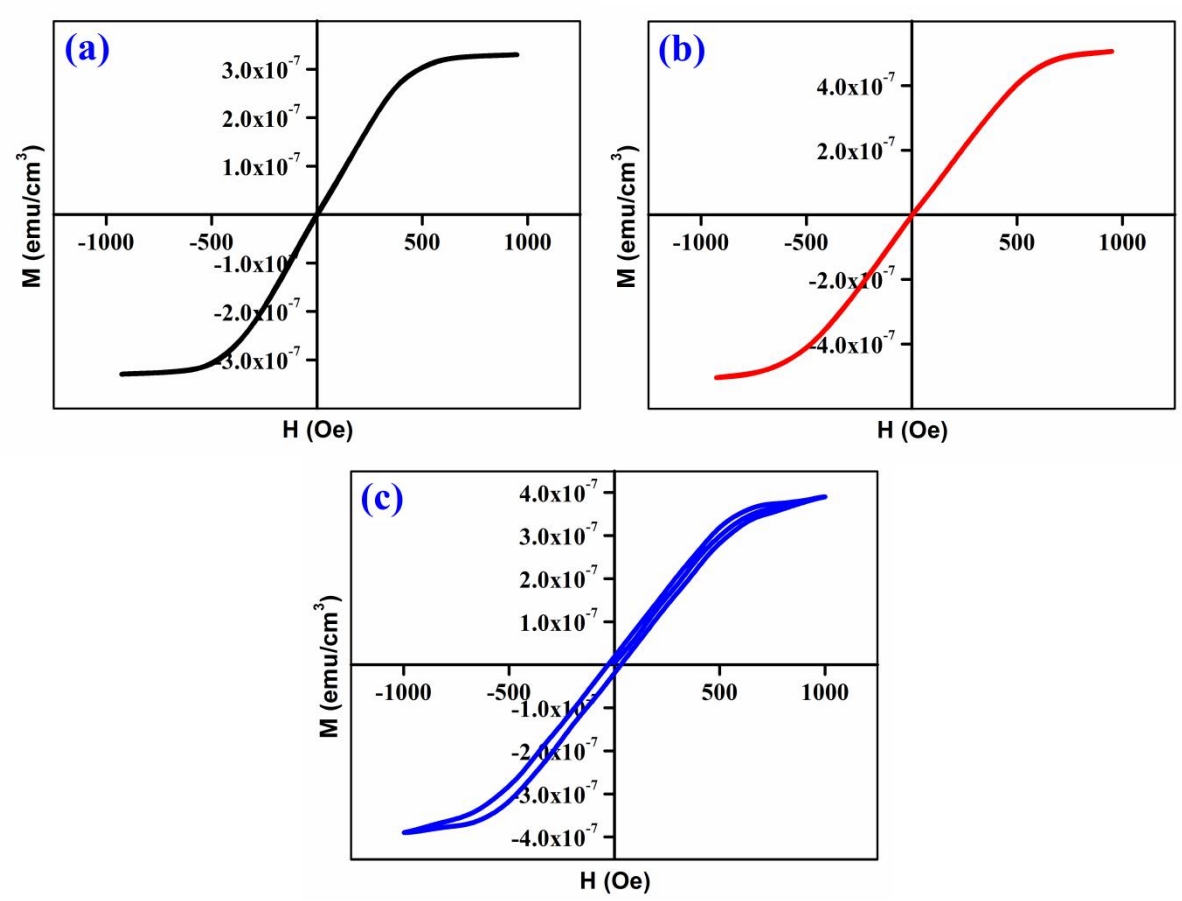

Fig 9.U, M and ML's M-H spectra

The ML film exhibited ferromagnetic ordering characterized by a distinct hysteresis loop. CdO's paramagnetic nature observed here matched with earlier results [23]. The saturation magnetization values of U, M and ML were 3.2, 5.6 and 3.7 x 10^{-7} emu/cm^3, respectively. M's increased saturation magnetization resulted from anti-ferromagnetic coupling between Mg^{2+} ions due to super-exchange interactions [24]. The ferromagnetic interactions between Li^{+}ions, which took the role of Cd^{2+} in the CdO lattice, may be the cause of the ferromagnetic orderings observed in the ML film [25]. Point defects related to cadmium and oxygen might have also contributed to the ferromagnetism realized for the ML film. The distribution of cations on the A and B sites, as a result of exchange interaction, is another possible explanation for the observed ferromagnetism.Cd^{2+} and Mg^{2+}occupies tetrahedral A and octahedral B-sites, and Li^{+} ions occupy both tetrahedral and octahedral sites. As a result, dopants occupy Cd^{2+} ion sites, and A-B interaction strength rises, increasing saturation magnetisation and magnetic moments [26]. The retentivity and coercivity values obtained of the ML film were 1.96 x 10^{-6} emu/cm^3 and 32 Oe, respectively.

4. Conclusion

On glass substrates, undoped, Mg, and (Mg+Li) doped CdO thin films were deposited utilizing a spray approach with a perfume atomizer.XRD confirmed cubic nature preferentially oriented along the (1 1 1) plane. Increased transparency was realized for the Mg-doped and (Mg+Li) codoped CdO thin films. The codoped film had a low electrical resistance and a high figure of merit. Paramagnetic nature of CdO becomes ferromagnetic with (Mg+Li) codoping. Due to increased figure of merit value ($35.3\times 10^{-2}\ \Omega^{-1}$), the (Mg+Li) codoped CdO thin film is found suitable for optoelectronic applications.

Acknowledgments: Alagappa University, Karaikudi is very much appreciated for the XRD results.

Availability of Data and Materials: The datasets used and analyzed during the current study are available from the corresponding author on reasonable request.

Funding: This research received no external funding.

Author Contributions: ARB conceived and designed the research framework; RG carried out the experimental and computational work; TA provided critical guidance on the analytical methods and interpretation of results; SS performed the data analysis; ARB prepared the initial draft of the manuscript. All authors have read and approved the final manuscript. All authors contributed to editorial changes in the manuscript. All authors have participated sufficiently in the work and agreed to be accountable for all aspects of the work.

Conflicts of Interest: The authors declare no conflict of interest.

References

1. Sarath Babu, R.; Narasimha Murthy, Y.; Vinoth, S.; Rimal Isaac, R.S.; Mohanraj, P.; Ganesh, V.; Algarni, H.; AlFaify, S. Enhancement in optoelectronic properties of lanthanum co-doped CdO:Zn thin films for TCO applications. *Superlattices and Microstructures* 2022, 162, 107097. https://doi.org/10.1016/j.spmi.2021.107097.

2. Kabir, M.H.; Hafiz, M.; Urmi, S.A.; Haque, M.J.; Ali, M.M.; Rahman, Md.S.; Khan, M.K.R.; Rahman, M.S. Effect of Ga doping on microstructure, morphology, optical and electrical properties of spray deposited CdO thin films. *Optical Materials* 2022, 125, 112123. https://doi.org/10.1016/j.optmat.2022.112123.

3. Munawar, T.; Nadeem, M.S.; Mukhtar, F.; Manzoor, S.; Naeem Ashiq, M.; Batool, S.; Hasan, M.; Iqbal, F. Enhanced photocatalytic, antibacterial, and electrochemical properties of CdO based nanostructures by transition metals codoping. *Advanced Powder Technology* 2022, 33(3), 103451. https://doi.org/10.1016/j.apt.2022.103451.

4. Usharani, K.; Balu, A.R.; Nagarethinam, V.S.; Suganya, M. Characteristic analysis on the physical properties of nanostructured Mg-doped CdO thin films – Doping concentration effect. *Progress in Natural Science: Materials International* 2015, 25(3), 251 – 257. https://doi.org/10.1016/j.pnsc.2015.06.003.

5. Antosoly, D.; Ilangovan, S.; Suganya, M.; Balamurugan, S.; Balu, A.R. Optical and magnetic properties of CdO thin films doped with Ba^{2+} ions. *Materials Research Innovations* 2018, 22(6), 237–241. https://doi.org/10.1080/14328917.2017.1303015.

6. Yahia, I.S.; Salem, G.F.; Iqbal, J.; Yakuphanoglu, F. Linear and nonlinear optical discussions of nanostructured Zn-doped CdO thin films. *Physica B: Condensed Matter* 2017, 511, 54 – 60. https://doi.org/10.1016/j.physb.2017.01.030.

7. Ashaduzzman, M.; Khan, M.K.R.; Karim, A.M.M.T.; Rahman, M.M. Influence of chromium on structural, nonlinear optical constants and transport properties of CdO thin films. *Surfaces and Interfaces* 2018, 12, 135 – 141. https://doi.org/10.1016/j.surfin.2018.05.008.

8. Gupta, R.K.; Serbetci, Z.; Yakuphanoglu, F. Bandgap variation in size-controlled nanostructured Li – Ni codoped CdO thin films. *Journal of Alloys and Compounds* 2012, 515, 96 – 100. https://doi.org/10.1016/j.jallcom.2011.11.098.

9. Aydin, R.; Sahin, B. Comprehensive research on physical properties of Zn and M (M: Li, Na, K) doubledopedcadmium oxide (CdO) nanostructures using SILAR method. *Ceramics International* 2017, 43(12), 9285 – 9290. https://doi.org/10.1016/j.ceramint.2017.04.087.

10. Dakhel, A.A. Near-infrared transparent conducting CdO nanocrystalline films codoped with boron and hydrogen. *Current Applied Physics* 2012, 12(1), 1 – 6. https://doi.org/10.1016/j.cap.2011.04.016.

11. Samiyammal, P.; Parasuraman, K.; Balu, A.R. Doping effects investigation of Li-doped CdS thin films. *Surface Engineering* 2019, 35(1), 79 – 85. https://doi.org/10.1080/02670844.2018.1473198.

12. Xu, Z.Q.; Deng, H.; Li, Y.; Guo, Q.H.; Li, Y.R. Characteristics of Al-doped c-axis oriented ZnO thin films prepared by sol – gel method. *Materials Research Bulletin* 2006, 41(2), 354 – 358. https://doi.org/10.1016/j.materresbull.2005.08.014.

13. Manna, S.; Chan, H.; Ghosh, A.; Chakrabarti, T.; Sankaranarayanan, K.R.S. Understanding and control of Zener pinning via phase field and ensemble learning. *Computational Materials Science* 2023, 229, 112384. https://doi.org/10.1016/j.commatsci.2023.112384.

14. Hassanzadeh-Tabrizi, S.A. Precise calculation of crystallite size of nanomaterials: A review. *Journal of Alloys and Compounds* 2023, 968, 171914. https://doi.org/10.1016/j.jallcom.2023.171914.

15. Balaji, R.; Mohan, P.; Vinoth, S.; Hadi, M.; Ashraf, I.M.; Ansari, K.B.; Khan, M.T.; Sangaraju, S.; Shkir, M. Fascinating opto-gas sensors development based on$Ti_{1-x}Er_xO_2$thin films for environmental and optoelectronic devices. *Journal of Science: Advanced Materials and Devices* 2026, 11(1), 101096. https://doi.org/10.1016/j.jsamd.2026.101096.

16. Khan, Z.R.; Alshammari, A.S.; Shkir, M.; Bouzidi, M.; Mohamed, M.; Kumar, M.; Sonker, R.K. Effect of Ag doping on structural, morphological and optical properties of CdO nanostructured thin films. Physica B: Condensed Matter 2022, 632, 413762. https://doi.org/10.1016/j.physb.2022.413762.

17. Hassan, A.; Jin, Y.; Irfan, M.; Jiang, Y. Acceptor-modulated optical enhancements and band gap narrowing in ZnO thin films. AIP Advances 2018, 8(3), 035212. https://doi.org/10.1063/1.5020830.

18. Shanmugavel, G.; Balu, A.R.; Nagarethinam, V.S.; Ravishankar, S.; Suganya, M.; Balamurugan, S.; Usharani, K.; Kayathiri, C.; Karthika, M. CdO:Ag thin films with enhanced visible-light photocatalytic activity against metanil yellow. *SN Applied Sciences* 2019, 1, 1203. https://doi.org/10.1007/s42452-019-1237-2.

19. Kennedy, A.; Ganesan, H.; Marnadu, R.; Karthik Kannan, S.; Arockiam, S.I.; Ubaidullah, M.; Shkir, M.; Alfaify, S.; Gedi, S. An effect of metal ions (Cu, Mn) doping on the structural, morphological, optical, photoluminescence, electric and photocatalytic properties of In_2S_3 nanoparticles. *Optical Materials* 2022, 124, 111769. https://doi.org/10.1016/j.optmat.2021.111769.

20. Abed, H.R.; Khudadad, A.I.; Yousif, A.A. Impact of high vacuum annealing temperature on the structural, photoluminescence, and room temperature liquefied petroleum gas sensing of direct current magnetron sputtered CdO films. *Materials Chemistry and Physics* 2022, 289, 126446. https://doi.org/10.1016/j.matchemphys.2022.126446.

21. Suganya, M.; Balu, A.R.; Prabha, D.; Anitha, S.; Balamurugan, S.; Srivind, J. PbS – SnO_2 nanocomposite with enhanced magnetic, photocatalytic and antifungal properties. *Journal of Materials Science: Materials in Electronics* 2018, 29, 1065 – 1974. https://doi.org/10.1007/s10854-017-8007-y.

22. Mohamed, S.H.; Hadia, H.M.A.; Diab, A.K.; Abdel Hakeem, A.M. Synthesis, photoluminescence and optical constants evaluations of ultralong CdO nanowires prepared by vapour transport method. *Journal of Alloys and Compounds* 2014, 609, 68 – 72. https://doi.org/10.1016/j.jallcom.2014.04.065.

23. Karim, I.; Haque Naeem, M.A.; Rahman Ayon, A.S.; Sattar, Md.A.; Sabur, Md.A.; Ahmed, N.A. Effect of silver and cobalt on transparent conducting CdO thin films: tuning the optoelectronic properties. *Materials Advances* 2025, 6(2), 703 – 718. https://doi.org/10.1039/D4MA00918E

24. Sambasivam, S.; Joseph, D.P.; Tin, J.G.; Venkateswaran, C. Doping-induced magnetism in Co-doped ZnS nanoparticles. *Journal of Solid State Chemistry* 2009, 182(10), 2598 – 2601. https://doi.org/10.1016/j.jssc.2009.07.015.

25. Krasilnikov, V.; Zhukov, V.; Chulkov, E.; Tyutyunnik, A.; Dyachkova, T.; Baklanova, I.; Gyrdasova, O.; Zhuravlev, N.; Chistyakov, V.; Gao, T.; Eisterer, M.; Marchenkov, V. Precursor synthesis and properties of iron and lithium codoped cadmium oxide. *Journal of Electroceramics* 2022, 48(3), 127 – 142. https://doi.org/10.1007/s10832-022-00278-7.

26. Bammannavar, B.K.; Naik, L.R.; Pujar, R.B.; Chougule, B.K. Preparation, characterization and physical properties of Mg – Zn ferrites. *Indian Journal of Engineering & Materials Sciences* 2007, 14(5), 381 – 385.